Atmos. Meas. Tech. Discuss., 5, 4495–4534, 2012
www.atmos-meas-tech-discuss.net/5/4495/2012/
doi:10.5194/amtd-5-4495-2012

Atmospheric Measurement Techniques Discussions

Profiling tropospheric CO_2 using the Aura TES and TCCON instruments

L. Kuai[1], J. Worden[1], S. Kulawik[1], K. Bowman[1], S. Biraud[2], J. B. Abshire[3], S. C. Wofsy[4], V. Natraj[1], C. Frankenberg[1], D. Wunch[5], B. Connor[6], C. Miller[1], C. Roehl[5], R.-L. Shia[5], and Y. Yung[5]

[1]Jet Propulsion Laboratory, California Institute of Technology, 4800 Oak Grove Drive, Mail stop: 233-200, Pasadena, CA 91109, USA
[2]Lawrence Berkeley National Laboratories, Berkeley, CA, 94720, USA
[3]NASA Goddard Space Flight Center, Greenbelt, MD, USA
[4]Harvard University, Cambridge, MA, USA
[5]California Institute of Technology, 1200 E. California Blvd., Pasadena, CA, 91125, USA
[6]BC Consulting Ltd., 6 Fairway Dr, Alexandra, 9320, New Zealand

Received: 30 May 2012 – Accepted: 6 June 2012 – Published: 29 June 2012

Correspondence to: L. Kuai (lkuai@jpl.nasa.gov)

Published by Copernicus Publications on behalf of the European Geosciences Union.

Abstract

Monitoring the global distribution and long-term variations of CO_2 sources and sinks is required for characterizing the global carbon budget. Although total column measurements will be useful for estimating large regional fluxes, model transport error remains a significant error source, particularly for local sources and sinks. To improve the capability of estimating regional fluxes, we estimate near-surface CO_2 values from ground-based near infrared (NIR) measurements with space-based thermal infrared (TIR) measurements. The NIR measurements are obtained from the Total Carbon Column Observing Network (TCCON) of solar measurements which provide an estimate of the total CO_2 atmospheric column amount. Estimates of tropospheric CO_2 that are co-located with TCCON are obtained by assimilating Tropospheric Emission Spectrometer (TES) free-tropospheric CO_2 estimates into the GEOS-Chem model. Estimates of the boundary layer CO_2 are obtained through simple subtraction, as the CO_2 estimation problem is linear.

We find that the calculated random uncertainties in total column and boundary layer estimates are consistent with actual uncertainties as compared to aircraft data. For the total column estimates the random uncertainty is about 0.55 ppm with a bias of −5.66 ppm, consistent with previously published results. After accounting for the total column bias, the bias in the boundary layer CO_2 estimates is 0.26 ppm with a precision of 1.02 ppm This precision is sufficient for capturing the winter to summer variability of approximately 12 ppm in the lower troposphere; double the variability of the total column. This work shows that a combination of NIR and IR measurements can profile CO_2 with the precisions and accuracy needed to quantify near-surface CO_2 variability.

1 Introduction

Our ability to infer surface carbon fluxes depends critically on interpreting spatial and temporal variations of atmospheric CO_2 and relating them back to surface fluxes. For

AMTD
5, 4495–4534, 2012

example, surface CO_2 fluxes are typically calculated using surface or near surface CO_2 measurements along with aircraft data (Baker et al., 2010; Bousquet et al., 2000; Chevallier et al., 2010, 2011; Gurney et al., 2002; Keppel-Aleks et al., 2012; Law and Rayner, 1999; Rayner et al., 2008, 2011; Rayner and O'Brien, 2001). More recently it has been shown that total column CO_2 measurements derived from ground-based or satellite observations can be used to place constraints on continental-scale flux estimates (Chevallier, 2007; Chevallier et al., 2011; Keppel-Aleks et al., 2012; O'Brien and Rayner, 2002). However, because CO_2 is a long-lived greenhouse gas, measurements of the total column CO_2 is primarily sensitive to synoptic scale fluxes as discussed in Baker et al. (2010) and Keppel-Aleks et al. (2011); it is shown that variations in the total column are only partly driven by local surface fluxes because the total column also varies related to the transport of CO_2 from remote locations. Furthermore, the variations caused by the surface source and sinks are largest in the planetary boundary layer (PBL) CO_2 (Keppel-Aleks et al., 2011, 2012; Sarrat et al., 2007). In addition, Stephen et al. (2007) concludes that most of the current models overpredicts the annual-mean midday vertical gradients and consequently lead to an overestimated carbon uptake in northern lands and underestimated carbon uptake over tropical forests. For these reasons we could expect that vertical profile estimates of CO_2 will improve constraints on the distributions of carbon flux. Therefore, we are motivated to derive a method to estimate the PBL CO_2 from current available column and free tropospheric observations.

Total column CO_2 data are calculated from solar near infrared (NIR) measurements from the Total Carbon Column Observatory Network (TCCON) (Wunch et al., 2010, 2011a), as well as the space-borne instruments, starting from GOSAT (Crisp et al., 2004; O'Dell et al., 2012; Wunch et al., 2011b; Yokota et al., 2009; Yoshida et al., 2009). Similar space-borne instruments include OCO-2 which is expected to be launched this decade (Crisp et al., 2004), Carbonsat (Velazco et al., 2011) and GOSAT-2 (Yokota et al., 2009; Yoshida et al., 2009), which are also expected to be launched in near future. The ground-based measurements have high precision and accuracy but limited

AMTD
5, 4495–4534, 2012

spatial coverage. Satellite observations have lower precision and accuracy relative to the ground-based data, but obtain global measurements of atmospheric CO_2. In addition, there are free tropospheric CO_2 measurements from satellite instruments such as TES (Kulawik et al., 2010, 2012) and AIRS (Chahine et al., 2005).

In this paper, we present a method to estimate the PBL CO_2 by combining column and free tropospheric CO_2 from two data sources: total column estimates from TCCON and free tropospheric estimates from TES data, assimilated into the GEOS-Chem model. We do not use the direct profiling approach discussed in Christi and Stephens (2004) because we found that spectroscopic errors and sampling error due to poor co-location of the NIR and IR data currently result in unphysical retrieved CO_2 profiles. Instead we simply subtract free tropospheric column estimates from total column estimates in order to quantify lower tropospheric CO_2 column amounts. As long as the retrievals converge and the estimated states are close to the true states, the problem of subtracting free tropospheric column amount from total column amount is a linear problem with well characterized uncertainties.

2 Measurements

2.1 Ground-based total column CO_2 measurements from TCCON

The column data used to derive PBL CO_2 in this study are from TCCON observations. TCCON is a Fourier Transform Spectrometer instrument, with a precise solar tracking system. It measures incoming sunlight with high spectral resolution ($0.02\,cm^{-1}$) and high signal to noise ratio (SNR) between 500 and 885, depending on the spectral region observed (Washenfelder et al., 2006). The recorded spectral region ranges from 4000 to $15\,000\,cm^{-1}$. It provides a long-term observation of column-averaged abundance of greenhouse gases, such as CO_2, CH_4 N_2O and other trace gases (e.g., CO) over twenty TCCON sites around the world including both operational and future sites (Deutscher et al., 2010; Messerschmidt et al., 2011; Washenfelder et al., 2006; Wunch

AMTD
5, 4495–4534, 2012

et al., 2010; Yang et al., 2002). Figure 1 shows a measurement at 1.6 µm CO_2 absorption band, which is used for analysis here.

As discussed in Wunch et al. (2010; 2011a), total column-averaged abundances using TCCON data can be estimated using a non-linear least squares approach that compares a forward model spectrum that depends on CO_2, temperature, H_2O, and instrument parameters against the observed spectrum. The retrieval approach adjusts atmospheric CO_2 concentrations by scaling an a priori CO_2 profile until the observed and modeled spectra agree within the noise levels. The precision in the column-averaged CO_2 dry air mole fraction from the scaling retrievals is better than 0.25 % (Wunch et al., 2010, 2011a). The absolute accuracy is ~ 1 % and after calibration by aircraft data, it can reach 0.25 % (Wunch et al., 2010, 2011a).

In this paper, we use a profile retrieval algorithm that scales multiple levels of the CO_2 profile instead of the whole profile. We find that the precision of retrieved column averages of the profile using this approach (0.55 ppm) is consistent with the scaling retrievals described by Wunch et al. (2010). The profile retrieval algorithm is described in Sect. 4.

2.2 Satellite-based free tropospheric CO_2 measurements from TES

Free tropospheric CO_2 estimates are derived from thermal IR radiances measured by the Aura Tropospheric Emission Spectrometer (TES) (Beer et al., 2001). The TES instrument measures the infrared radiance emitted by Earth's surface and atmospheric gases and particles from space. These measurements have peak sensitivity to the mid-tropospheric CO_2 at ~ 500 hPa (Kulawik et al., 2012). Because the sampling for the TES CO_2 measurements is sparse (e.g., 1 measurement every 100 km approximately) and passing over the Lamont TCCON site ~ every 16 days, we assimilated the CO_2 measurements into the GEOS-Chem model, a global 3-D chemical transport model (CTM) (Beer et al., 2001; Kulawik et al., 2010, 2011; Nassar et al., 2010). We use the results from the assimilation as our free-tropospheric estimates of CO_2. Details of the assimilation approach are discussed in the Appendix (A5) and uncertainties in

AMTD
5, 4495–4534, 2012

the assimilation fields are calculated by comparison to aircraft data as discussed in Sect. 5.2.

2.3 Flight measurements

Aircraft data are used as our standard to assess the quality of the different CO_2 estimates. The aircraft measure CO_2 profiles typically up to 6 km and sometimes to 10 km or higher. For comparison with the TCCON CO_2 estimates, we collected profile observations from different aircraft campaigns, such as HIPPO (Wofsy et al., 2011) and Learjet (Abshire et al., 2010) (http://www.esrl.noaa.gov/gmd/ccgg/aircraft/qc.html), at the Southern Great Plains (SGP) ARM site (Kulawik et al., 2010, 2012) over the year 2009 (http://www.arm.gov/campaigns/aaf2008acme). These data are compared to the TCCON CO_2 observations at the Lamont site, Oklahoma (36.6° N, 97.5° W).

3 Calculation of column and PBL CO_2

The approach discussed in this paper is to estimate PBL CO_2 by subtracting estimates of free tropospheric CO_2 partial column amount from the total column amount. The total column amount is usually obtained by integrating the gas concentration profile from the surface to the top of atmosphere.

$$C_g = \int_{p_s}^{0} f_g^{dry}(p) \cdot \rho(p) \cdot dp \quad (1)$$

where C_g is total vertical column amount for gas "g" and $\rho(p)$ represents the number density vertical profile and $f_g^{dry}(p)$ is dry-air gas concentration profile as a function of

AMTD
5, 4495–4534, 2012

pressure (p).

$$f_g^{dry}(p) = \frac{f_g(p)}{1 - f_{H_2O}(p)} \quad (2)$$

The ratio of the total column between gas and air will give the dry-air column-averaged abundance, e.g., for CO_2:

$$XCO2 = \frac{C_{CO_2}}{C_{air}} \quad (3)$$

Here we use XCO2 to refer to dry-air column-averaged mole fraction of CO_2.

Since TCCON also provides precise measurements of O_2, dividing by the retrieved O_2 using spectral measurements from the same instrument improves the precision of XCO2 by significantly reducing the effects of instrumental or measurement errors that are common in both gases (e.g., solar tracker pointing errors, zero level offsets, instrument line shape errors, etc.) (Wunch et al., 2010). Therefore, we also remove the water fraction by normalizing simultaneously retrieved O_2. Because we retrieve the CO_2 profile, we can remove the water component layer by layer.

$$f_{CO_2}^{dry}(p) = \frac{f_{CO_2}(p)}{f_{O_2}(p)} \times 0.2095 \quad (4)$$

Then the column amount (C_{CO_2}) and the column average (XCO2) can be computed using Eqs. (1) and (3), respectively.

Consistent with the discussions in Wunch et al. (2010) the precision of column estimates using O_2 as the dry air standard will be improved but the bias specific from the use of the O_2 band will be transferred to XCO2. For example, Fig. 2 shows total column XCO2 estimates, retrieved from our algorithm, corresponding to aircraft in which data was taken from the surface past 10 km. The bias is found to negligibly vary over time and over different sites as discussed in Wunch et al. (2010).

AMTD
5, 4495–4534, 2012

Because O_2 normalized estimates of XCO2 have higher precision but about 1 % negative bias, we need to remove the mean bias in TCCON XCO2 when estimating the total column amount:

$$C_{CO_2} = C_{air}\left(\frac{XCO2^{TCCON}}{\alpha}\right) \quad (5)$$

where α is a correction factor to remove the bias in TCCON column retrievals.

The partial vertical column amount of CO_2 in free troposphere and above ($C_{CO_2}^{TROP}$) is estimated by integrating TES GEOS-Chem assimilated profile ($f_{CO_2}^{TES}$) above the boundary layer (600 hPa).

$$C_{CO_2}^{TROP} = \int_{600}^{0} f_{CO_2}^{TES}(p)\cdot\rho(p)\cdot dp \quad (6)$$

The partial vertical column amount of CO_2 in the PBL can then be computed as the difference between the total column amount (Eq. 5) and partial free tropospheric column amount (Eq. 6):

$$C_{CO_2}^{PBL} = C_{air}\left(\frac{XCO2^{TCCON}}{\alpha}\right) - \int_{600}^{0} f_{CO_2}^{TES}(p)\cdot\rho(p)\cdot dp \quad (7)$$

Applying Eq. (3) within the boundary layer gives the estimate of the PBL CO_2 mole fraction ($XCO2^{PBL}$), the ratio of partial vertical column between CO_2 ($C_{CO_2}^{PBL}$) and air ($C_{air}^{PBL} = \int_{p_s}^{600} 1\cdot\rho(p)\,dp$) is

$$XCO2^{PBL} = \frac{\frac{XCO2^{TCCON}}{\alpha}\int_{p_s}^{0} 1\cdot\rho(p)\cdot dp - \int_{600}^{0} f_{CO_2}^{TES}(p)\cdot\rho(p)\cdot dp}{\int_{p_s}^{600} 1\cdot\rho(p)\cdot dp} \quad (8)$$

AMTD
5, 4495–4534, 2012

where $XCO2^{PBL}$ is defined as the TCCON/TES PBL CO_2. These estimates can be compared to the integrated partial column-averaged CO_2 measured by aircraft within the boundary layer (surface to 600 hPa for Lamont).

4 CO_2 profile retrieval approach

In this section, we describe a profile retrieval algorithm that is based on the scaling retrieval discussed in Wunch et al. (2011a; 2010). Characterization of the errors, based on this retrieval approach, is discussed in the Appendix. The profile of atmospheric CO_2 is obtained by optimal estimation (Rodgers, 2000) using the same line-by-line radiative transfer model discussed in Wunch et al. (2010) (or GFIT). It computes simulated spectra using 71 vertical levels with 1 km intervals for the input atmospheric state (e.g., CO_2, H_2O, HDO, CH_4, O_2, P, T and etc.). The details about the TCCON instrument setup and GFIT are also described in Deutscher et al. (2010); Geibel et al. (2010); Washenfelder et al., (2006); Wunch et al. (2011a; 2010); Yang et al. (2002). The retrievals in this study use one of TCCON-measured CO_2 absorption bands, centered at 6220.00 cm^{-1} with a window width of 80.00 cm^{-1} (Fig. 1). Note that ultimately we do not use the full profiles for this study as we find that spectroscopic or other errors introduce jack-knifing into the estimated profiles with a variability that is larger than expected from comparison to aircraft data. Instead the profiles are mapped into column amounts and are shown to be consistent with the results of Wunch et al. (2011a). We use the profile retrieval instead of the Wunch et al. (2010) column scaling retrieval in order to understand the error characteristics of the CO_2 retrieval.

In the scaling retrieval discussed by Wunch et al. (2011a; 2010), the retrieved state vector ($\boldsymbol{\gamma}$) includes the eight constant scaling factors for four absorption gases (CO_2, H_2O, HDO, and CH_4) and four instrument parameters (continuum level: "cl", continuum

AMTD
5, 4495–4534, 2012

tilt: “ct”, frequency shift: “fs”, and zero level offset: “zo”).

$$\boldsymbol{\gamma} = \begin{bmatrix} \gamma_{[CO_2]} \\ \gamma_{[H_2O]} \\ \gamma_{[HDO]} \\ \gamma_{[CH_4]} \\ \gamma_{cl} \\ \gamma_{ct} \\ \gamma_{fs} \\ \gamma_{zo} \end{bmatrix} \quad (9)$$

Each element of $\boldsymbol{\gamma}$ is a ratio between the state vector ($\boldsymbol{x}$) and its a priori ($\boldsymbol{x}_a$). In the profile retrieval, for the target gas CO_2, we estimate the altitude dependent scaling factors instead. For other interfering gases, a single scaling factor is retrieved. Ten levels are chosen for CO_2 (see Fig. 3a) to capture its vertical variation:

$$\boldsymbol{\gamma} = \begin{bmatrix} \gamma_{1[CO_2]} \\ \vdots \\ \gamma_{10[CO_2]} \\ \gamma_{[H_2O]} \\ \gamma_{[HDO]} \\ \gamma_{[CH_4]} \\ \gamma_{cl} \\ \gamma_{ct} \\ \gamma_{fs} \\ \gamma_{zo} \end{bmatrix} \quad (10)$$

To obtain a concentration profile, the retrieved scaling factors need to be mapped from retrieval grids (i.e., 10 levels for CO_2 and 1 level for other three gases) to the 71 forward model levels.

$$\boldsymbol{\beta} = \mathbf{M}\boldsymbol{\gamma} \quad (11)$$

AMTD
5, 4495–4534, 2012

where $\mathbf{M} = \frac{\partial \boldsymbol{\beta}}{\partial \boldsymbol{\gamma}}$ is a linear mapping matrix relating retrieval level to the forward model altitude grid. Multiplying the scaling factor ($\boldsymbol{\beta}$) on the forward model level to $\mathbf{M}_x = \frac{\partial \boldsymbol{x}}{\partial \boldsymbol{\beta}}$, a diagonal matrix of the concentration a priori ($\boldsymbol{x}_a$) gives the true state of gas profile:

$$\boldsymbol{x} = \mathbf{M}_x \boldsymbol{\beta} \tag{12}$$

According to the above definition, the a priori profile is $\boldsymbol{x}_a = \mathbf{M}_x \boldsymbol{\beta}_a$ and estimated state is $\hat{\boldsymbol{x}} = \mathbf{M}_x \hat{\boldsymbol{\beta}}$.

The non-linear least square retrieval also depends on a constraint matrix to regularize choices for the retrieval solution (Bowman et al., 2006). The non-diagonal CO_2 covariance matrix used to generate the constraint matrix has larger variance in the boundary layer and decreases with altitude. This covariance is generated using the GEOS-Chem model as guidance. However, we scale the diagonals of the covariance matrix in order to match the variability observed at the TCCON sites. The square root of the diagonal of this covariance is approximately 2 % in the boundary layer, 1 % in the free troposphere, and less than 1 % in the stratosphere (Fig. 3a). The off-diagonal correlations are shown in Fig. 3b.

The measurement noise, or signal-to-noise (SNR) is used to weight the measurement relative to the a priori in the non-linear least squares retrieval. Although the SNR of the TCCON instrument is better than 500, we use a SNR of approximately 200 because spectroscopic uncertainties degrade the comparison (O'Dell et al., 2011; Wunch et al., 2011a); use of this SNR results in a chi-square in our retrievals of about 1.

To obtain the best estimate of the state vector that minimize the difference between the observed spectral radiances ($\boldsymbol{y}_o$) and the forward model spectral radiances ($\boldsymbol{y}_m$) we perform Bayesian optimization by minimizing the cost function, $\chi(\boldsymbol{\gamma})$:

$$\chi(\boldsymbol{\gamma}) = (\boldsymbol{y}_m - \boldsymbol{y}_o)^T \mathbf{S}_e^{-1} (\boldsymbol{y}_m - \boldsymbol{y}_o) + (\boldsymbol{\gamma} - \boldsymbol{\gamma}_a)^T \mathbf{S}_a^{-1} (\boldsymbol{\gamma} - \boldsymbol{\gamma}_a) \tag{13}$$

where $\mathbf{S}_a$ is chosen to be the covariance shown in Fig. 3 and $\mathbf{S}_e$ is the measurement noise covariance, a diagonal matrix with values of noise squared

AMTD
5, 4495–4534, 2012

5 Results

5.1 Quality of the column-averaged CO_2 estimates

To characterize the quality of the CO_2 estimates, we compare the TCCON column-averaged estimates with the aircraft column-integrated data. Calculated errors (as derived in the Appendix) are compared to actual errors as derived empirically from comparison of the estimates to the aircraft data and are shown to be consistent.

There are forty-one SGP aircraft measured CO_2 profiles in 2009 (Fig. 4). Most aircraft measurements are from the surface to 6 km; however, three profiles have measurements from the surface to 10 km or higher (31 July, 2 and 3 August). To estimate the total column (or), the CO_2 values for altitudes above the top of the aircraft measurements are replaced by the TCCON CO_2 a priori, shifted to match the value at the top of the aircraft measurements. As discussed in the Appendix (A1.2.1), this approximation to the upper tropospheric CO_2 values negligibly contributes to uncertainty in the comparison between TCCON XCO2 estimates and the aircraft + shifted upper troposphere a priori profiles. The comparisons between TCCON column averages and the derived aircraft column averages are summarized in Fig. 5 and Table 1.

TCOON XCO2 estimates are calculated within a 4-h time window, centered about the time corresponding to each aircraft profile. A 4-h time window is chosen to ensure that comparisons are statistically meaningful and also to ensure that variations in CO_2 and temperature are small relative to calculated uncertainties. Comparisons between TCCON and aircraft XCO2 are shown in Table 1. Results listed in Table 1 are only for clear-sky scenes because it is difficult to quantify the effect of clouds on the TCCON retrievals and errors. We find that the calculated precision for the collection of measurements within each 4-h time window encompassing the aircraft is, on average, approximately 0.32 ppm. This precision is, on average, consistent with the variability of the TCCON XCO2 estimates within this 4-h time window of 0.35 ppm. The error on the mean will be arbitrarily small because of the large number of measurements within this 4-h time window. Consequently, we expect that the XCO2 variability within each

AMTD
5, 4495–4534, 2012

4-h time window is driven by noise but not by variations in temperature and CO_2. However, we calculate that errors in temperature lead to an error in XCO2 of approximately 0.69 ppm on average (last column, Table 1). We find that the TCCON XCO2 estimates are biased on average by -5.66 ± 0.55 ppm. The magnitude of this bias estimate is consistent with that described in Wunch et al. (2010) and is attributed to errors in the O_2 spectroscopy. The error in the bias (0.55 ppm) is consistent with the calculated error due to temperature (0.69 ppm) and is a result of temperature variations between aircraft measurements.

5.2 Quality of the PBL CO_2 estimates

In this section we examine the robustness of estimates of XCO2 in the PBL (surface to 600 hPa) by comparison of the TCCON/TES XCO2 estimates to aircraft data. We separate the boundary layer from the free-troposphere at the 600 hPa pressure level because the aircraft profiles indicate that the variability in the free troposphere becomes "small" above this pressure (Fig. 4). However, knowledge of the boundary layer height will affect use of these PBL estimates for quantifying surface fluxes because boundary layer heights are typically at higher pressures than 600 hPa (von Engeln et al., 2005) Figure 6a shows comparisons of the PBL XCO2 as calculated from integrating a priori profiles used with GFIT from surface to 600 hPa. Figure 6b shows comparisons of the PBL XCO2 as calculated from TCCON and TES data. The -5.66 ppm bias (or factor α in Eq. 9) is removed from the TCCON total column before computing XCO2 in the PBL using TCCON data and TES data. As shown in Table 2, the averaged difference between aircraft and TCCON/TES PBL XCO2 values is 0.26 ± 1.02 ppm. The averaged difference between TES (assimilated into GEOS-Chem) free tropospheric CO_2 (above 600 hPa) and aircraft free tropospheric CO_2 is 0.38 ± 0.71 ppm. According to Appendix A2 (Eq. A28), the estimated uncertainty in PBL XCO2 by TCCON/TES is 0.90 ppm, consistent with actually uncertainty of 1.02 ppm. The improvement in this lower tropospheric XCO2 comparison, relative to the a priori, is mainly during summer time when surface CO_2 is low, relative to wintertime, because the biosphere is more

AMTD
5, 4495–4534, 2012

active in the summer (Fig. 6). With these uncertainties, the PBL XCO2 estimates are able to capture the seasonal variability of the lower troposphere as discussed next.

5.3 Seasonal variability of PBL CO_2 compared to column CO_2

The aircraft, TCCON, and TES assimilated estimates of atmospheric CO_2 have sufficient temporal density to provide an estimate of CO_2 variability over most of the year. In Figure 7 we show the monthly averaged total column averages and the partial column averages (surface to 600 hPa) calculated from the aircraft data and the same quantities derived from the TCCON data and the TCCON minus TES assimilated data, respectively. The TCCON column averages (black dots) and TCCON/TES derived PBL data (red dots) are consistent with the aircraft measurement (black diamonds and red diamonds) within the expected uncertainties indicating that the estimates are robust. Based on these forty-one flight profiles, there are about 3 to 5 days to be averaged in each month of the year except September and October, both of which only have one available aircraft profile and are happen to under unclear sky scenes. Therefore, the comparisons for these two months are not shown. Both TCCON column averages and TCCON/TES PBL CO_2 capture the seasonal variability.

The response of the seasonal variability in PBL CO_2 is more than twice that in the column averages. It is 14 ppm peak-to-peak in PBL CO_2 and 5 ppm in the column-averaged CO_2 because there is a rapid drawdown in PBL CO_2 at the growing season onset over mid latitude due to the biosphere uptake. The difference between the PBL CO_2 and column CO_2 changes from positive (about 3 ppm) to negative (lower than −4 ppm) over the year (Fig. 7b). It suggests that the processes driving the surface fluxes at Lamont are different than the processes driving the total column. Consequently, these results empirically indicate that these estimated PBL CO_2 will provide improved sensitivity to local fluxes than the total column (Keppel-Aleks et al., 2011).

AMTD
5, 4495–4534, 2012

6 Summary

Total column estimates of atmospheric CO_2 and partial column estimates of CO_2 in the boundary layer (surface to 600 hPa) are calculated using TCCON and Aura TES data. In order to determine if the retrieval approach, forward model, and understanding of uncertainties are robust, it is crucial to determine if the calculated uncertainties are consistent with the actual uncertainties. In addition, we need to assess any biases in the estimates and ideally attribute these bias errors in the measurement system. The bias and its uncertainties in TCCON column-averaged CO_2 are explained at two different time scales: 4-h time windows centered about individual aircraft measurement and day-to-day time scales from comparison to the collection of forty-one aircraft profiles. We find that for multiple retrievals of the same air parcel within a 4-h time window, the mean bias is from the uncertainties of atmospheric states (i.e., temperature or interference gases) or spectroscopy parameters. The variability of the collection of total column estimates within the 4-h time window of 0.35 ppm is consistent with the calculated random error of about 0.32 ppm, which is associated with the measurement error. When comparing the TCCON total column estimates to aircraft data over several days, we can assume that the daily systematic errors due to temperature or other interference error is pseudo-random. For example, the estimated mean bias across multiple days is −5.66 (±0.55) ppm. The standard deviation of the bias error of approximately 0.55 ppm is consistent with the expected error of 0.69 ppm, which is primarily driven by temperature error; measurement error for these comparisons is arbitrarily small because of the large number of measurements used to calculate the mean CO_2 estimate.

Comparisons of the aircraft data to free tropospheric CO_2 calculated by assimilating Aura TES CO_2 estimates into the GEOS-Chem model (Nassar et al., 2011) suggest that the TES assimilated data has a bias error of 0.38 (±0.71) ppm in the free troposphere. We calculated a boundary layer estimate (surface to 600 hPa) of the CO_2 amount by subtracting the TES assimilated free tropospheric estimate from the TCCON total column amount estimates. Comparisons of these boundary layer estimates

AMTD
5, 4495–4534, 2012

from TCCON/TES data to those from aircraft data are consistent after the bias in the TCCON is removed. The precision in the derived PBL CO_2 is 1.02 ppm, which is consistent with the calculated precision of 0.90 ppm. The dominant sources of the error in the PBL estimates are due to uncertainties in the free troposphere data from TES assimilation and the temperature driven error in column averages from TCCON. We show that this precision is sufficient to characterize the seasonal boundary layer variability of CO_2 over the TCCON sites.

This study highlights the potential of combining simultaneous measurements from near IR and IR sounding instruments to obtain vertical information of the CO_2 profile (Christi and Stephens, 2004). The present TCCON network is relatively sparse but has a good latitudinal coverage and long-term accurate observations of column abundance of CO_2. Column estimates of CO_2 by space measurement are currently available from GOSAT and SCIAMACHY data (Schneising et al., 2011, 2012) and are expected from OCO-2. Column CO_2 estimates from these satellite data together with the free tropospheric CO_2 estimates are anticipated to provide complementary constraints to infer CO_2 fluxes and advance the ability to study the carbon cycle problem by providing constraints on near-surface CO_2 variations and atmospheric mixing.

Appendix A

Error characterization

A1 Errors in TCCON column-averaged CO_2

In this section, we develop the error characterization for (1) the estimates of TCCON CO_2 column averages from the profile retrievals for a 4-h time window around each aircraft CO_2 profile measurement and (2) comparisons of TCCON estimates against forty-one aircraft profiles.

AMTD
5, 4495–4534, 2012

As discussed in the text (Sect. 4), the retrieval vector is defined by:

$$\boldsymbol{\gamma} = \begin{bmatrix} \gamma_{1[CO_2]} \\ \vdots \\ \gamma_{10[CO_2]} \\ \gamma_{[H_2O]} \\ \gamma_{[HDO]} \\ \gamma_{[CH_4]} \\ \gamma_{cl} \\ \gamma_{ct} \\ \gamma_{fs} \\ \gamma_{zo} \end{bmatrix} \tag{A1}$$

Each element of $\boldsymbol{\gamma}$ is a ratio between the state vector ($\boldsymbol{x}$) and its a priori ($\boldsymbol{x}_a$). For the target gas CO_2, altitude dependent scaling factors are retrieved. For other interferential gases, a constant scaling factor for the whole profile is retrieved. The last four are for the instrument parameters (continuum level: "cl", continuum title: "ct", frequency shift: "fs", and zero level offset: "zo"). To obtain a concentration profile, the retrieved scaling factors are mapped from the retrieval grid (i.e., 10 levels for CO_2 and 1 level for other three gases) to the 71 forward model levels.

$$\boldsymbol{\beta} = \mathbf{M}\boldsymbol{\gamma} \tag{A2}$$

where $\mathbf{M} = \frac{\partial \boldsymbol{\beta}}{\partial \boldsymbol{\gamma}}$ is a linear mapping matrix relating retrieval levels to the forward model altitude grid. Multiplying the scaling factor ($\boldsymbol{\beta}$) on the forward model level to the concentration a priori ($\boldsymbol{x}_a$) gives the estimates of the gas profile. We define $\mathbf{M}_x = \frac{\partial \boldsymbol{x}}{\partial \boldsymbol{\beta}}$ where $\mathbf{M}_x$ is a diagonal matrix filled by the concentration a priori ($\boldsymbol{x}_a$):

$$\hat{\boldsymbol{x}} = \mathbf{M}_x \hat{\boldsymbol{\beta}} \tag{A3}$$

AMTD
5, 4495–4534, 2012

From Eq. (A3), it follows that $\boldsymbol{x}_a = \mathbf{M}_x\boldsymbol{\beta}_a$ and $\boldsymbol{x} = \mathbf{M}_x\boldsymbol{\beta}$ The Jacobian matrix of retrieved parameter with respect to the radiance is

$$\mathbf{K}_\gamma = \frac{\partial \mathbf{L}(\mathbf{M}\boldsymbol{\gamma})}{\partial \boldsymbol{\gamma}} \tag{A4}$$

Using the chain rule, we can obtain the equation relating the retrieval Jacobians to the full-state Jacobian

$$\frac{\partial \mathbf{L}}{\partial \boldsymbol{\gamma}} = \frac{\partial \mathbf{L}}{\partial \boldsymbol{x}}\frac{\partial \boldsymbol{x}}{\partial \boldsymbol{\beta}}\frac{\partial \boldsymbol{\beta}}{\partial \boldsymbol{\gamma}} \tag{A5}$$

or

$$\mathbf{K}_\gamma = \mathbf{K}_x\mathbf{M}_x\mathbf{M} = \mathbf{K}_\beta\mathbf{M} \tag{A6}$$

If the estimated state is "close" to the true state, then the estimated state for a single measurement can be expressed as a linear retrieval equation (Rodgers, 2000):

$$\hat{\boldsymbol{\beta}} = \boldsymbol{\beta}_a + \mathbf{A}_\beta(\boldsymbol{\beta} - \boldsymbol{\beta}_a) + \mathbf{M}\mathbf{G}_\gamma\boldsymbol{\varepsilon}_n + \sum_l \mathbf{M}\mathbf{G}_\gamma\mathbf{K}_b^l\Delta\boldsymbol{b}^l \tag{A7}$$

where $\boldsymbol{\varepsilon}_n$ is a zero-mean noise vector with covariance $\mathbf{S}_e$ and the vector $\Delta\boldsymbol{b}^l$ is the error in true state of parameters (l) that also affect the modeled radiance, e.g., temperature, interfering gases, spectroscopy. The $\mathbf{K}_b^l$ is the Jacobian of parameter (l). In this study, we found the systematic error is primarily due to the temperature uncertainty ($\boldsymbol{\varepsilon}_T$) and spectroscopic error ($\boldsymbol{\varepsilon}_L$) $\mathbf{G}_\gamma$ is the gain matrix, which is defined by

$$\mathbf{G}_\gamma = \frac{\partial \boldsymbol{\gamma}}{\partial \mathbf{L}} = (\mathbf{K}_\gamma^T\mathbf{S}_e^{-1}\mathbf{K}_\gamma + \mathbf{S}_a^{-1})^{-1}\mathbf{K}_\gamma^T\mathbf{S}_e^{-1} \tag{A8}$$

The averaging kernel for $\boldsymbol{\beta}$ in forward model dimension is

$$\mathbf{A}_\beta = \mathbf{M}\mathbf{G}_\gamma\mathbf{K}_\beta \tag{A9}$$

AMTD
5, 4495–4534, 2012

We can define $\mathbf{A}_x = \mathbf{M}_x\mathbf{A}_\beta\mathbf{M}_x^{-1}$ as the averaging kernel for $\boldsymbol{x}$. In order to convert Eq. (A7) to the state vector of concentration ($\hat{\boldsymbol{x}}$) we apply Eq. (A7) into Eq. (A3) and obtain:

$$\hat{\boldsymbol{x}} = \boldsymbol{x}_a + \mathbf{A}_x(\boldsymbol{x}-\boldsymbol{x}_a) + \mathbf{M}_x\mathbf{M}\mathbf{G}_\gamma\boldsymbol{\varepsilon}_n + \mathbf{M}_x\mathbf{M}\mathbf{G}_\gamma\mathbf{K}_T\boldsymbol{\varepsilon}_T + \mathbf{M}_x\mathbf{M}\mathbf{G}_\gamma\mathbf{K}_L\boldsymbol{\varepsilon}_L \quad \text{(A10)}$$

The temperature uncertainty ($\boldsymbol{\varepsilon}_T$) and spectroscopic error ($\boldsymbol{\varepsilon}_L$) represent the systematic errors ($\boldsymbol{\Delta b}'$).

A2 Total error budget

The error for a single retrieval is

$$\delta\hat{\boldsymbol{x}} = \hat{\boldsymbol{x}}-\boldsymbol{x} = (\mathbf{I}-\mathbf{A}_x)(\boldsymbol{x}_a-\boldsymbol{x}) + \mathbf{M}_x\mathbf{M}\mathbf{G}_\gamma\boldsymbol{\varepsilon}_n+\mathbf{M}_x\mathbf{M}\mathbf{G}_\gamma\mathbf{K}_T\boldsymbol{\varepsilon}_T + \mathbf{M}_x\mathbf{M}\mathbf{G}_\gamma\mathbf{K}_L\boldsymbol{\varepsilon}_L \quad \text{(A11)}$$

The second order statistics for the error is

$$\mathbf{S}_{\delta\hat{\boldsymbol{x}}} = \hat{\mathbf{S}}_{sm} + \hat{\mathbf{S}}_m+\hat{\mathbf{S}}_T+\hat{\mathbf{S}}_L \quad \text{(A12)}$$

where the smoothing error covariance is

$$\hat{\mathbf{S}}_{sm} = (\mathbf{I}-\mathbf{A}_x)\mathbf{S}_a(\mathbf{I}-\mathbf{A}_x)^T \quad \text{(A13)}$$

a measurement error covariance is

$$\hat{\mathbf{S}}_m = \mathbf{M}_x\mathbf{M}\mathbf{G}\mathbf{S}_e(\mathbf{M}_x\mathbf{M}\mathbf{G})^T \quad \text{(A14)}$$

and two systematic error covariance matrices are

$$\hat{\mathbf{S}}_T = \mathbf{M}_x\mathbf{M}\mathbf{G}\mathbf{K}_T\mathbf{S}_T(\mathbf{M}_x\mathbf{M}\mathbf{G}\mathbf{K}_T)^T \quad \text{(A15)}$$

$$\hat{\mathbf{S}}_L = \mathbf{M}_x\mathbf{M}\mathbf{G}\mathbf{K}_L\mathbf{S}_L(\mathbf{M}_x\mathbf{M}\mathbf{G}\mathbf{K}_L)^T \quad \text{(A16)}$$

$\mathbf{S}_a$ is the a priori covariance for CO_2, $\mathbf{S}_e$ is the covariance describing the TCCON measurement noise, $\mathbf{S}_T$ is the a priori covariance for temperature and is based on the a priori covariance used for the Aura TES temperature retrievals (Worden et al., 2004); this temperature covariance is based on the expected uncertainty in the reanalysis fields that are inputs to the TES retrievals. $\mathbf{S}_L$ is the covariance associated with spectroscopic error.

AMTD
5, 4495–4534, 2012

A3 Individual error budget terms

For comparisons of TCCON retrievals to each aircraft profile we choose the TCCON measurements taken within a 4-h time window centered about the aircraft measurement. This time window is short enough so that we can assume the atmospheric state has not changed but it is also long enough that there are enough samples of retrievals for good statistics (e.g., ∼ 100 samples).

There are forty-one aircraft measurements that measured CO_2 profiles over Lamont in 2009. On any given day (or ith day), we have n_i TCCON retrievals within a 4-h time window around aircraft measurement where n_i varies by day (or by aircraft profile comparison). The difference of the mean of these retrievals to the aircraft measurement is the error on that day. The average of the errors from these forty-one comparison estimates the mean bias error. Which term contributes to the uncertainties will be discuss in follow.

A3.1 Error due to extrapolation of CO_2 above aircraft profile

In reality, the true state ($\boldsymbol{x}$) is unknown and can only be estimated by our best measurements, such as by aircraft, which have a precision of 0.02 ppm. With the validation standard, the error in the retrieval ($\delta\hat{\boldsymbol{x}}$) can be estimated by the comparison of the retrieved state vector ($\hat{\boldsymbol{x}}$) to the validation standard ($\hat{\boldsymbol{x}}_{\text{std}}$). In order to do an inter-comparison of the measurements from two different instruments, we apply a smoothing operator described in Rodgers and Connor (2003) to the complete profile ($\boldsymbol{x}_{\text{FLT}}$) based on aircraft measurement so that it is smoothed by the averaging kernel and a priori constraint from the TCCON profile retrieval:

$$\hat{\boldsymbol{x}}_{\text{std}} = \boldsymbol{x}_{\text{a}} + \mathbf{A}_{\boldsymbol{x}}\left(\boldsymbol{x}_{\text{FLT}} - \boldsymbol{x}_{\text{a}}\right) \tag{A17}$$

$\hat{\boldsymbol{x}}_{\text{std}}$ is the profile that would be retrieved from TCCON measurements for the same air sampled by the aircraft without the presence of other errors. $\boldsymbol{x}_{\text{FLT}}$ is the complete CO_2 profile based on aircraft measurement.

AMTD
5, 4495–4534, 2012

Several aircraft only measure CO_2 up to approximately 6 km, but three of them go up to 10 km or higher. Therefore, the lower part of $\boldsymbol{x}_{\mathrm{FLT}}$ is from the direct aircraft measurements. Above that, the TCCON a priori is scaled to the CO_2 values at the top of the aircraft measurement so that the profile is continuously extended up to 71 km. We use this approximation because the free tropospheric CO_2 is well mixed (vertical variations in free troposphere is less than 1 ppm) (Wofsy et al., 2011). Then the complete profile based on the aircraft measurement is

$$\boldsymbol{x}_{\mathrm{FLT}} = \begin{bmatrix} \boldsymbol{x}_{\mathrm{FLT}}^{\mathrm{meas}} \\ \lambda \boldsymbol{x}_{\mathrm{a}}^{f} \end{bmatrix} = \boldsymbol{x} - \delta \boldsymbol{x}_{\mathrm{FLT}} = \boldsymbol{x} - \begin{bmatrix} \delta \boldsymbol{x}_{\mathrm{FLT}}^{\mathrm{meas}} \\ \boldsymbol{x}^{f} - \lambda \boldsymbol{x}_{\mathrm{a}}^{f} \end{bmatrix} \tag{A18}$$

where $\boldsymbol{x}_{\mathrm{FLT}}^{\mathrm{meas}}$ is the direct aircraft measurements in the lower atmosphere, which has been mapped to forward model grid. $\delta \boldsymbol{x}_{\mathrm{FLT}}^{\mathrm{meas}}$ is its unknown error relative to the "truth" and is order of 0.02 ppm. λ is the ratio between the CO_2 at the top of aircraft measurement to the a priori CO_2 on that level. $\boldsymbol{x}_{\mathrm{a}}^{f}$ and $\boldsymbol{x}^{f}$ represent the a priori and "true" state above direct aircraft measurement in the free troposphere and above. $\lambda \boldsymbol{x}_{\mathrm{a}}^{f}$ is the shifted a priori to smoothly extend the profile up to stratosphere. $\boldsymbol{x}_{\mathrm{FLT}}$ represents the complete profile based combining a priori.

Subtracting Eq. (A17) from Eq. (A10) results in the following expression:

$$\delta \hat{\boldsymbol{x}} = \hat{\boldsymbol{x}} - \hat{\boldsymbol{x}}_{\mathrm{std}} = \mathbf{A}_{\boldsymbol{x}} \delta \boldsymbol{x}_{\mathrm{FLT}} + \mathbf{M}_{\boldsymbol{x}} \mathbf{M} \mathbf{G}_{\boldsymbol{y}} \boldsymbol{\varepsilon}_{n} + \mathbf{M}_{\boldsymbol{x}} \mathbf{M} \mathbf{G}_{\boldsymbol{y}} \mathbf{K}_{T} \boldsymbol{\varepsilon}_{T} + \mathbf{M}_{\boldsymbol{x}} \mathbf{M} \mathbf{G}_{\boldsymbol{y}} \mathbf{K}_{L} \boldsymbol{\varepsilon}_{L} \tag{A19}$$

The second order statistics for the error in the complete aircraft based profile, $\delta \boldsymbol{x}_{\mathrm{FLT}}$, is:

$$\mathbf{S}_{\delta \boldsymbol{x}_{\mathrm{FLT}}} = \mathbf{E}[\delta \boldsymbol{x}_{\mathrm{FLT}} - \mathbf{E}(\delta \boldsymbol{x}_{\mathrm{FLT}})][\delta \boldsymbol{x}_{\mathrm{FLT}} - \mathbf{E}(\delta \boldsymbol{x}_{\mathrm{FLT}})]^{T} = \begin{bmatrix} \mathbf{S}_{\mathrm{FLT}}^{\mathrm{meas}} & \mathbf{0} \\ \mathbf{0} & \mathbf{S}_{\mathrm{a}}^{f} \end{bmatrix} \tag{A20}$$

$\mathbf{S}_{\mathrm{FLT}}^{\mathrm{meas}}$ is the error covariance for direct aircraft measurements, which is a diagonal matrix with a constant value of the square of 0.02 ppm (the accuracy of aircraft instruments). $\mathbf{S}_{\mathrm{a}}^{f}$ is the sub matrix of TCCON a priori covariance matrix above the aircraft

AMTD
5, 4495–4534, 2012

measurements. Since we scale the a priori to the aircraft data, the actual error covariance in the upper atmosphere should be much smaller than $\mathbf{S}_{\mathrm{a}}^{f}$.

The uncertainty in retrieved column averages driven by the smoothing error can be estimated by

$$\sigma_{\mathrm{sm}}(\delta\mathrm{XCO2}) = \sqrt{\boldsymbol{h}^{T}\mathbf{A}_{\boldsymbol{x}}\mathbf{S}_{\delta\boldsymbol{x}_{\mathrm{FLT}}}\mathbf{A}_{\boldsymbol{x}}^{T}\boldsymbol{h}} \tag{A21}$$

The upper limit of this uncertainty is approximately 0.5 ppm when using the a priori covariance in the upper atmosphere where the aircraft measurement is missing (e.g., above 6 km). Since the free troposphere is well mixed and the upper atmosphere is constrained by the aircraft measurement, the actual uncertainty for the validation standard should be much smaller than above estimates. For example, if we assume conservatively that the term, $\mathbf{S}_{\delta\boldsymbol{x}_{\mathrm{FLT}}}$, is half the size of the $\mathbf{S}_{\mathrm{a}}$ used to describe our CO_2 covariance, then this term becomes negligible relative to the temperature error.

A3.2 Measurement error

The measurement noise vector $\boldsymbol{\varepsilon}_{n}$ is a zero-mean random variable. In a 4-h time window, the measurement error covariance will drive the variability of the retrieved column averages. The uncertainty in retrieved column averages driven by the measurement error can be estimated by

$$\sigma_{\mathrm{m}}(\delta\mathrm{XCO2}) = \sqrt{\boldsymbol{h}^{T}\hat{\mathbf{S}}_{\mathrm{m}}\boldsymbol{h}} \tag{A22}$$

$\hat{S}_{\mathrm{m}}$ is defined in Eq. (A14). We calculate that this term is approximately 0.32 ppm. The error on the mean is related to the number of samples in 4-h time window:

$$\sigma_{\mathrm{m}}(\delta\mathrm{XCO2}) = \sqrt{\frac{\boldsymbol{h}^{T}\hat{S}_{\mathrm{m}}\boldsymbol{h}}{n_{i}}} \tag{A23}$$

where n_{i} is number of retrieval samples within 4-h on ith day (listed in Table 1).

AMTD
5, 4495–4534, 2012

A3.3 Temperature error

Within a 4-h time window, we assume that variations in temperature do not result in variations in the CO_2 estimate; however, the uncertainty in the temperature profiles will result in a bias:

$$\overline{(\delta \mathrm{XCO2})_{T_i}} = \boldsymbol{h}^T \mathbf{M}_x \mathbf{M} \mathbf{G}_\gamma \mathbf{K}_T \boldsymbol{\varepsilon}_{T_i} \tag{A24}$$

However, $\boldsymbol{\varepsilon}_{T_i}$ varies from day to day. The mean bias error from temperature uncertainties over days becomes

$$\overline{(\delta \mathrm{XCO2})_T} = \boldsymbol{h}^T \mathbf{M}_x \mathbf{M} \mathbf{G}_\gamma \mathbf{K}_T \left(\frac{1}{m} \sum_{i=1}^{m} \boldsymbol{\varepsilon}_{T_i} \right) \tag{A25}$$

with a covariance of

$$\sigma_T(\delta \mathrm{XCO2}) = \sqrt{\boldsymbol{h}^T \hat{S}_T \boldsymbol{h}} \tag{A26}$$

where $\hat{S}_T$ is from Eq. (A15). The estimate of this term is, on average, approximately 0.69 ppm.

A3.4 Spectroscopic error

The spectroscopic error is another significant source of systematic error. Different from temperature error, it does not vary significantly on any time scales and even over different sites (Wunch et al., 2010). Therefore, its covariance is always negligible. However, it is found to be the primary source of the bias error.

$$\overline{(\delta \mathrm{XCO2})_L} = \boldsymbol{h}^T \mathbf{M}_x \mathbf{M} \mathbf{G}_\gamma \mathbf{K}_L \boldsymbol{\varepsilon}_L \tag{A27}$$

The estimate of this term is about −5 ppm. It is mainly due to the error in O_2 cross section.

AMTD
5, 4495–4534, 2012

A4 Errors in PBL column-averaged CO_2

We estimate the PBL CO_2 by subtracting the TES assimilated free tropospheric CO_2 from the TCCON total column CO_2. The TCCON dry-air total column estimated by weighted to the retrieved O_2 column has a bias of approximately −5.66 ppm. Therefore, we remove the bias using Eq. (5) before subtracting the free tropospheric partial column amount. Because the TCCON estimates and TES/GEOS-Chem estimates are independent estimates of CO_2, the uncertainties in the boundary layer estimates are simply the uncertainties summed in quadrature:

$$\sigma\left(\delta X_{CO_2}^{PBL}\right) = \sqrt{\sigma^2\left(\delta X_{CO_2}^{TES}\right) + \sigma^2\left(\delta X_{CO_2}^{TCCON}\right)} \tag{A28}$$

The estimate of this term is 0.90 ppm. The TES assimilated free tropospheric bias error and uncertainty is estimated by the comparison to the free tropospheric estimates from the aircraft-based profile ($\boldsymbol{x}_{FLT}$). The TCCON total column mean bias error and uncertainty has been discussed in previous section Eqs. (A27) and (A26).

A5 Estimating the free tropospheric CO_2 column using TES and GEOS-Chem

To estimate the free tropospheric CO_2, retrieved TES CO_2 fields are assimilated into the GEOS-Chem model. GEOS-Chem is a global 3-D chemical transport model (CTM) for atmospheric composition, with sources and additional modifications specific to the carbon cycle as described in (Nassar et al., 2010) and (Kulawik et al., 2011). TES at all pressure levels between 40° S and 40° N, along with the predicted sensitivity and errors, was assimilated for the year 2009 using 3d-var assimilation. We compare model output with and without assimilation to surface based in situ aircraft measurements from the US DOE Atmospheric Radiation Measurement (ARM) Southern Great Plains site during the ARM-ACME (www.arm.gov/campaigns/aaf2008acme) and HIPPO-2 (hippo.ucar.edu/) mission (Kulawik et al., 2012). We find improvement in the seasonal cycle amplitude in the mid-troposphere at the SGP site, but also discrepancies with

AMTD
5, 4495–4534, 2012

HIPPO at remote oceanic sites, particularly outside of the latitude range of assimilation (Kulawik et al., 2012).

Supplementary material related to this article is available online at: http://www.atmos-meas-tech-discuss.net/5/4495/2012/amtd-5-4495-2012-supplement.pdf.

Acknowledgement. Part of this research was carried out at the Jet Propulsion Laboratory, California Institute of Technology, under a contract with the National Aeronautics and Space Adminisotration. The GEOS-Chem model results with assimilated TES data was funded by proposal No. 09-ACOS09-0010. US funding for TCCON comes from NASA's Terrestrial Ecology Program, grant number NNX11AG01G, the Orbiting Carbon Observatory Program, the Atmospheric CO_2 Observations from Space (ACOS) Program and the DOE/ARM Program. SGP data was supported by the Office of Biological and Environmental Research of the US Department of Energy under contract No. DE-AC02-05CH11231 as part of the Atmospheric Radiation Measurement Program. The authors wish to thank G. Toon and P. Wennberg for making available their GFIT code and TCCON data.

References

Abshire, J. B., Riris, H., Allan, G. R., Weaver, C. J., Mao, J. P., Sun, X. L., Hasselbrack, W. E., Kawa, S. R., and Biraud, S.: Pulsed airborne lidar measurements of atmospheric CO_2 column absorption, Tellus B, 62, 770–783, 2010.

Baker, D. F., Bösch, H., Doney, S. C., O'Brien, D., and Schimel, D. S.: Carbon source/sink information provided by column CO_2 measurements from the Orbiting Carbon Observatory, Atmos. Chem. Phys., 10, 4145–4165, doi:10.5194/acp-10-4145-2010, 2010.

Beer, R., Glavich, T. A., and Rider, D. M.: Tropospheric emission spectrometer for the Earth Observing System's Aura Satellite, Appl. Opt., 40, 2356–2367, 2001.

Bousquet, P., Peylin, P., Ciais, P., Le Quere, C., Friedlingstein, P., and Tans, P. P.: Regional changes in carbon dioxide fluxes of land and oceans since 1980, Science, 290, 1342–1346, 2000.

AMTD
5, 4495–4534, 2012

Bowman, K. W., Rodgers, C. D., Kulawik, S. S., Worden, J., Sarkissian, E., Osterman, G., Steck, T., Lou, M., Eldering, A., Shephard, M., Worden, H., Lampel, M., Clough, S., Brown, P., Rinsland, C., Gunson, M., and Beer, R.: Tropospheric emission spectrometer: retrieval method and error analysis, IEEE T. Geosci. Remote, 44, 1297–1307, 2006.

Chahine, M., Barnet, C., Olsen, E. T., Chen, L., and Maddy, E.: On the determination of atmospheric minor gases by the method of vanishing partial derivatives with application to CO_2, Geophys. Res. Lett., 32, L22803, doi:10.1029/2005GL024165, 2005.

Chevallier, F.: Impact of correlated observation errors on inverted CO_2 surface fluxes from OCO measurements, Geophys. Res. Lett., 34, L24804, doi:10.1029/2007gl030463, 2007.

Chevallier, F., Ciais, P., Conway, T. J., Aalto, T., Anderson, B. E., Bousquet, P., Brunke, E. G., Ciattaglia, L., Esaki, Y., Frohlich, M., Gomez, A., Gomez-Pelaez, A. J., Haszpra, L., Krummel, P. B., Langenfelds, R. L., Leuenberger, M., Machida, T., Maignan, F., Matsueda, H., Morgui, J. A., Mukai, H., Nakazawa, T., Peylin, P., Ramonet, M., Rivier, L., Sawa, Y., Schmidt, M., Steele, L. P., Vay, S. A., Vermeulen, A. T., Wofsy, S., and Worthy, D.: CO_2 surface fluxes at grid point scale estimated from a global 21 year reanalysis of atmospheric measurements, J. Geophys. Res.-Atmos., 115, D21307, doi:10.1029/2010jd013887, 2010.

Chevallier, F., Deutscher, N. M., Conway, T. J., Ciais, P., Ciattaglia, L., Dohe, S., Frohlich, M., Gomez-Pelaez, A. J., Griffith, D., Hase, F., Haszpra, L., Krummel, P., Kyro, E., Labuschagne, C., Langenfelds, R., Machida, T., Maignan, F., Matsueda, H., Morino, I., Notholt, J., Ramonet, M., Sawa, Y., Schmidt, M., Sherlock, V., Steele, P., Strong, K., Sussmann, R., Wennberg, P., Wofsy, S., Worthy, D., Wunch, D., and Zimnoch, M.: Global CO_2 fluxes inferred from surface air-sample measurements and from TCCON retrievals of the CO_2 total column, Geophys. Res. Lett., 38, L24810, doi:10.1029/2011gl049899, 2011.

Christi, M. J. and Stephens, G. L.: Retrieving profiles of atmospheric CO_2 in clear sky and in the presence of thin cloud using spectroscopy from the near and thermal infrared: a preliminary case study, J. Geophys. Res.-Atmos., 109, D04316, doi:10.1029/2003JD004058, 2004.

Crisp, D., Atlas, R. M., Breon, F. M., Brown, L. R., Burrows, J. P., Ciais, P., Connor, B. J., Doney, S. C., Fung, I. Y., Jacob, D. J., Miller, C. E., O'Brien, D., Pawson, S., Randerson, J. T., Rayner, P., Salawitch, R. J., Sander, S. P., Sen, B., Stephens, G. L., Tans, P. P., Toon, G. C., Wennberg, P. O., Wofsy, S. C., Yung, Y. L., Kuang, Z. M., Chudasama, B., Sprague, G., Weiss, B., Pollock, R., Kenyon, D., and Schroll, S.: The orbiting carbon observatory (OCO) mission, Trace Constit. Troposph. Lower Stratosph., 34, 700–709, 2004.

AMTD
5, 4495–4534, 2012

Deutscher, N. M., Griffith, D. W. T., Bryant, G. W., Wennberg, P. O., Toon, G. C., Washenfelder, R. A., Keppel-Aleks, G., Wunch, D., Yavin, Y., Allen, N. T., Blavier, J.-F., Jiménez, R., Daube, B. C., Bright, A. V., Matross, D. M., Wofsy, S. C., and Park, S.: Total column CO_2 measurements at Darwin, Australia – site description and calibration against in situ aircraft profiles, Atmos. Meas. Tech., 3, 947–958, doi:10.5194/amt-3-947-2010, 2010.

Geibel, M. C., Gerbig, C., and Feist, D. G.: A new fully automated FTIR system for total column measurements of greenhouse gases, Atmos. Meas. Tech., 3, 1363–1375, doi:10.5194/amt-3-1363-2010, 2010.

Gurney, K. R., Law, R. M., Denning, A. S., Rayner, P. J., Baker, D., Bousquet, P., Bruhwiler, L., Chen, Y. H., Ciais, P., Fan, S., Fung, I. Y., Gloor, M., Heimann, M., Higuchi, K., John, J., Maki, T., Maksyutov, S., Masarie, K., Peylin, P., Prather, M., Pak, B. C., Randerson, J., Sarmiento, J., Taguchi, S., Takahashi, T., and Yuen, C. W.: Towards robust regional estimates of CO_2 sources and sinks using atmospheric transport models, Nature, 415, 626–630, 2002.

Keppel-Aleks, G., Wennberg, P. O., and Schneider, T.: Sources of variations in total column carbon dioxide, Atmos. Chem. Phys., 11, 3581–3593, doi:10.5194/acp-11-3581-2011, 2011.

Keppel-Aleks, G., Wennberg, P. O., Washenfelder, R. A., Wunch, D., Schneider, T., Toon, G. C., Andres, R. J., Blavier, J.-F., Connor, B., Davis, K. J., Desai, A. R., Messerschmidt, J., Notholt, J., Roehl, C. M., Sherlock, V., Stephens, B. B., Vay, S. A., and Wofsy, S. C.: The imprint of surface fluxes and transport on variations in total column carbon dioxide, Biogeosciences, 9, 875–891, doi:10.5194/bg-9-875-2012, 2012.

Kulawik, S. S., Jones, D. B. A., Nassar, R., Irion, F. W., Worden, J. R., Bowman, K. W., Machida, T., Matsueda, H., Sawa, Y., Biraud, S. C., Fischer, M. L., and Jacobson, A. R.: Characterization of Tropospheric Emission Spectrometer (TES) CO_2 for carbon cycle science, Atmos. Chem. Phys., 10, 5601–5623, doi:10.5194/acp-10-5601-2010, 2010.

Kulawik, S. S., Bowman, K. W., Lee, M., Nassar, R., Jones, D. B. A., Biraud, S. C., Wofsy, S., Wunch, D., Gregg, W., Worden, J. R., and Frankenberg, C.: Constraints on near surface and free Troposphere CO_2 concentrations using TES and ACOS-GOSAT CO_2 data and the GEOS-Chem model, AGU presentation, 2011.

Kulawik, S. S., Worden, J. R., Wofsy, S. C., Biraud, S. C., Nassar, R., Jones, D. B. A., Olsen, E. T., and Osterman, and the TES and HIPPO teams, G. B.: Comparison of improved Aura Tropospheric Emission Spectrometer (TES) CO_2 with HIPPO and SGP aircraft profile measurements, Atmos. Chem. Phys. Discuss., 12, 6283–6329, doi:10.5194/acpd-12-6283-2012, 2012.

AMTD
5, 4495–4534, 2012

Law, R. M. and Rayner, P. J.: Impacts of seasonal covariance on CO_2 inversions, Global Biogeochem. Cy., 13, 845–856, 1999.

Messerschmidt, J., Geibel, M. C., Blumenstock, T., Chen, H., Deutscher, N. M., Engel, A., Feist, D. G., Gerbig, C., Gisi, M., Hase, F., Katrynski, K., Kolle, O., Lavrić, J. V., Notholt, J., Palm, M., Ramonet, M., Rettinger, M., Schmidt, M., Sussmann, R., Toon, G. C., Truong, F., Warneke, T., Wennberg, P. O., Wunch, D., and Xueref-Remy, I.: Calibration of TCCON column-averaged CO_2: the first aircraft campaign over European TCCON sites, Atmos. Chem. Phys., 11, 10765–10777, doi:10.5194/acp-11-10765-2011, 2011.

Nassar, R., Jones, D. B. A., Suntharalingam, P., Chen, J. M., Andres, R. J., Wecht, K. J., Yantosca, R. M., Kulawik, S. S., Bowman, K. W., Worden, J. R., Machida, T., and Matsueda, H.: Modeling global atmospheric CO_2 with improved emission inventories and CO_2 production from the oxidation of other carbon species, Geosci. Model Dev., 3, 689–716, doi:10.5194/gmd-3-689-2010, 2010.

Nassar, R., Jones, D. B. A., Kulawik, S. S., Worden, J. R., Bowman, K. W., Andres, R. J., Suntharalingam, P., Chen, J. M., Brenninkmeijer, C. A. M., Schuck, T. J., Conway, T. J., and Worthy, D. E.: Inverse modeling of CO_2 sources and sinks using satellite observations of CO_2 from TES and surface flask measurements, Atmos. Chem. Phys., 11, 6029–6047, doi:10.5194/acp-11-6029-2011, 2011.

O'Brien, D. M. and Rayner, P. J.: Global observations of the carbon budget – 2. CO_2 column from differential absorption of reflected sunlight in the 1.61 mum band of CO_2, J. Geophys. Res.-Atmos., 107, 4354, doi:10.1029/2001JD000617, 2002.

O'Dell, C. W., Day, J. O., Pollock, R., Bruegge, C. J., O'Brien, D. M., Castano, R., Tkatcheva, I., Miller, C. E., and Crisp, D.: Preflight radiometric calibration of the orbiting carbon observatory, IEEE T. Geosci. Remote, 49, 2438–2447, 2011.

O'Dell, C. W., Connor, B., Bösch, H., O'Brien, D., Frankenberg, C., Castano, R., Christi, M., Eldering, D., Fisher, B., Gunson, M., McDuffie, J., Miller, C. E., Natraj, V., Oyafuso, F., Polonsky, I., Smyth, M., Taylor, T., Toon, G. C., Wennberg, P. O., and Wunch, D.: The ACOS CO_2 retrieval algorithm – Part 1: Description and validation against synthetic observations, Atmos. Meas. Tech., 5, 99–121, doi:10.5194/amt-5-99-2012, 2012.

Rayner, P. J. and O'Brien, D. M.: The utility of remotely sensed CO_2 concentration data in surface source inversions (vol 28, pg 175, 2001), Geophys. Res. Lett., 28, 2429–2429, 2001.

Rayner, P. J., Law, R. M., Allison, C. E., Francey, R. J., Trudinger, C. M., and Pickett-Heaps, C.: Interannual variability of the global carbon cycle (1992–2005) inferred by inversion

AMTD
5, 4495–4534, 2012

of atmospheric CO_2 and $\delta_1 CO_2$ measurements, Global Biogeochem. Cy., 22, Gb3008, doi:10.1029/2007gb003068, 2008.
Rayner, P. J., Koffi, E., Scholze, M., Kaminski, T., and Dufresne, J. L., Constraining predictions of the carbon cycle using data, Philos. Trans. Roy. Soc. A, 369, 1955–1966, 2011.
Rodgers, C. D.: Inverse Methods for Atmospheric Sounding: Theory and Practice, World Scientific, London, 256 pp., 2000.
Sarrat, C., Noilhan, J., Lacarrere, P., Donier, S., Lac, C., Calvet, J. C., Dolman, A. J., Gerbig, C., Neininger, B., Ciais, P., Paris, J. D., Boumard, F., Ramonet, M., and Butet, A.: Atmospheric CO_2 modeling at the regional scale: Application to the CarboEurope Regional Experiment, J. Geophys. Res.-Atmos., 112, D12105, doi:10.1029/2006jd008107, 2007.
Schneising, O., Buchwitz, M., Reuter, M., Heymann, J., Bovensmann, H., and Burrows, J. P.: Long-term analysis of carbon dioxide and methane column-averaged mole fractions retrieved from SCIAMACHY, Atmos. Chem. Phys., 11, 2863–2880, doi:10.5194/acp-11-2863-2011, 2011.
Schneising, O., Bergamaschi, P., Bovensmann, H., Buchwitz, M., Burrows, J. P., Deutscher, N. M., Griffith, D. W. T., Heymann, J., Macatangay, R., Messerschmidt, J., Notholt, J., Rettinger, M., Reuter, M., Sussmann, R., Velazco, V. A., Warneke, T., Wennberg, P. O., and Wunch, D.: Atmospheric greenhouse gases retrieved from SCIAMACHY: comparison to ground-based FTS measurements and model results, Atmos. Chem. Phys., 12, 1527–1540, doi:10.5194/acp-12-1527-2012, 2012.
Stephens, B. B., Gurney, K. R., Tans, P. P., Sweeney, C., Peters, W., Bruhwiler, L., Ciais, P., Ramonet, M., Bousquet, P., Nakazawa, T., Aoki, S., Machida, T., Inoue, G., Vinnichenko, N., Lloyd, J., Jordan, A., Heimann, M., Shibistova, O., Langenfelds, R. L., Steele, L. P., Francey, R. J., and Denning, A. S.: Weak northern and strong tropical land carbon uptake from vertical profiles of atmospheric CO_2, Science, 316, 1732–1735, 2007.
Velazco, V. A., Buchwitz, M., Bovensmann, H., Reuter, M., Schneising, O., Heymann, J., Krings, T., Gerilowski, K., and Burrows, J. P.: Towards space based verification of CO_2 emissions from strong localized sources: fossil fuel power plant emissions as seen by a CarbonSat constellation, Atmos. Meas. Tech., 4, 2809–2822, doi:10.5194/amt-4-2809-2011, 2011.
von Engeln, A., Teixeira, J., Wickert, J., and Buehler, S. A.: Using CHAMP radio occultation data to determine the top altitude of the Planetary Boundary Layer, Geophys. Res. Lett., 32, L06815, doi:10.1029/2004gl022168, 2005.

AMTD
5, 4495–4534, 2012

Washenfelder, R. A., Toon, G. C., Blavier, J. F., Yang, Z., Allen, N. T., Wennberg, P. O., Vay, S. A., Matross, D. M., and Daube, B. C.: Carbon dioxide column abundances at the Wisconsin Tall Tower site, J. Geophys. Res.-Atmos., 111, D22305, doi:10.1029/2006jd007154, 2006.

Wofsy, S. C., the HIPPO Science Team, and Cooperating Modellers and Satellite Teams: HIAPER Pole-to-Pole Observations (HIPPO): fine-grained, global-scale measurements of climatically important atmospheric gases and aerosols, Philos. Trans. Roy. Soc. A, 369, 2073–2086, 2011.

Wunch, D., Toon, G. C., Wennberg, P. O., Wofsy, S. C., Stephens, B. B., Fischer, M. L., Uchino, O., Abshire, J. B., Bernath, P., Biraud, S. C., Blavier, J.-F. L., Boone, C., Bowman, K. P., Browell, E. V., Campos, T., Connor, B. J., Daube, B. C., Deutscher, N. M., Diao, M., Elkins, J. W., Gerbig, C., Gottlieb, E., Griffith, D. W. T., Hurst, D. F., Jiménez, R., Keppel-Aleks, G., Kort, E. A., Macatangay, R., Machida, T., Matsueda, H., Moore, F., Morino, I., Park, S., Robinson, J., Roehl, C. M., Sawa, Y., Sherlock, V., Sweeney, C., Tanaka, T., and Zondlo, M. A.: Calibration of the Total Carbon Column Observing Network using aircraft profile data, Atmos. Meas. Tech., 3, 1351–1362, doi:10.5194/amt-3-1351-2010, 2010.

Wunch, D., Toon, G. C., Blavier, J. F. L., Washenfelder, R. A., Notholt, J., Connor, B. J., Griffith, D. W. T., Sherlock, V., and Wennberg, P. O.: The Total Carbon Column Observing Network (TCCON), Philosophical Transactions of the Royal Society a-Mathematical Physical and Engineering Sciences, 369, 2087–2112, doi:10.1098/rsta.2010.0240, 2011a.

Wunch, D., Wennberg, P. O., Toon, G. C., Connor, B. J., Fisher, B., Osterman, G. B., Frankenberg, C., Mandrake, L., O'Dell, C., Ahonen, P., Biraud, S. C., Castano, R., Cressie, N., Crisp, D., Deutscher, N. M., Eldering, A., Fisher, M. L., Griffith, D. W. T., Gunson, M., Heikkinen, P., Keppel-Aleks, G., Kyrö, E., Lindenmaier, R., Macatangay, R., Mendonca, J., Messerschmidt, J., Miller, C. E., Morino, I., Notholt, J., Oyafuso, F. A., Rettinger, M., Robinson, J., Roehl, C. M., Salawitch, R. J., Sherlock, V., Strong, K., Sussmann, R., Tanaka, T., Thompson, D. R., Uchino, O., Warneke, T., and Wofsy, S. C.: A method for evaluating bias in global measurements of CO_2 total columns from space, Atmos. Chem. Phys., 11, 12317–12337, doi:10.5194/acp-11-12317-2011, 2011b.

Yang, Z. H., Toon, G. C., Margolis, J. S., and Wennberg, P. O.: Atmospheric CO_2 retrieved from ground-based near IR solar spectra, Geophys. Res. Lett., 29, 1339, doi:10.1029/2001GL014537, 2002.

AMTD
5, 4495–4534, 2012

Yokota, T., Yoshida, Y., Eguchi, N., Ota, Y., Tanaka, T., Watanabe, H., and Maksyutov, S.: Global concentrations of CO_2 and CH_4 retrieved from GOSAT: first preliminary results, Sola, 5, 160–163, doi:10.2151/sola.2009-041, 2009.

AMTD
5, 4495–4534, 2012

Table 1. Lists of bias error and its standard deviation ($1 \times \sigma$) of TCCON profile retrieved column averages within 4-h time window of each flight measurement. The expected uncertainties from measurement error covariance and the temperature error covariance are also listed in the last two columns. To remove the unclear sky spectra measurements, we dismiss the retrievals when the parameter "fvis" (fractional variation in solar intensity) is greater than 0.05, which suggests the cloud coverage during the spectra measurement. By applying the cloud filter, the consistency between the imperial error estimates and expected error estimates is improved. The columns for "n" are the total numbers of retrievals within 4-h time window.

Unit (ppm)	With cloud filter			Expected	
Day	Bias+5.66 (ppm)	Actual ($1 \times \sigma$)	n	$\sigma(\delta X^{h}_{CO_2})$	$\sigma(\delta X^{day}_{CO_2})$
8 January 2009	0.66	0.30	161	0.27	0.74
16 January 2009	0.45	0.30	171	0.33	0.74
29 January 2009	0.36	0.30	169	0.34	0.77
4 February 2009	0.58	0.26	169	0.33	0.74
11 February 2009	0.69	0.49	90	0.33	0.75
19 February 2009	0.39	0.38	96	0.33	0.76
21 February 2009	0.67	0.42	130	0.34	0.77
8 March 2009	0.25	0.39	132	0.32	0.71
14 March 2009	0.98	0.42	102	0.33	0.73
16 March 2009	0.00	0.27	154	0.32	0.69
18 March 2009	0.26	0.44	112	0.32	0.69
29 March 2009	−0.08	0.28	76	0.33	0.72
7 April 2009	0.13	0.26	98	0.33	0.72
8 April 2009	−0.03	0.40	121	0.32	0.69
20 April 2009	−0.59	0.44	69	0.32	0.70
21 April 2009	−0.32	0.29	130	0.32	0.70
23 April 2009	−0.21	0.30	122	0.32	0.66
17 May 2009	−0.19	0.32	130	0.32	0.70
18 May 2009	0.82	0.32	131	0.32	0.68
20 May 2009	0.60	0.50	75	0.32	0.67
26 May 2009	−0.12	0.36	86	0.32	0.67
28 May 2009	0.11	0.30	130	0.32	0.68
30 May 2009	0.30	0.34	130	0.32	0.66
4 June 2009	0.01	0.38	128	0.32	0.68
12 June 2009	−0.96	0.35	72	0.32	0.66
16 June 2009	−1.31	0.34	128	0.31	0.64
21 June 2009	−0.85	0.28	95	0.31	0.63
23 June 2009	−0.56	0.32	129	0.31	0.63
29 June 2009	0.16	0.32	118	0.31	0.64
1 July 2009	−0.24	0.46	119	0.31	0.65
6 July 2009	0.85	0.33	43	0.32	0.66
31 July 2009	0.31	0.34	125	0.32	0.66
2 August 2009	0.26	0.29	131	0.31	0.65
3 August 2009	−0.37	0.33	130	0.31	0.63
23 August 2009	−0.74	0.38	130	0.31	0.65
1 November 2009	−0.47	0.36	130	0.32	0.68
2 November 2009	−0.68	0.33	131	0.32	0.69
3 November 2009	−0.94	0.35	131	0.32	0.70
22 November 2009	−0.38	0.39	68	0.32	0.71
18 December 2009	−0.23	0.47	127	0.33	0.75
20 December 2009	0.33	0.38	101	0.33	0.72
Mean	0.00	0.35	118	0.32	0.69
$1 \times \sigma$	0.55				

AMTD
5, 4495–4534, 2012

Table 2. Bias and precision.

Unit (ppm)		Estimated bias	Precision
Total column averages	TCCON TCCON prior	−5.66 1.04	0.55 1.50
PBL column averages;	TCCON – TES/GEOS-Chem	0.26	1.02
Combining two data set; (total column amount – free troposphere column amount (above 600 hPa))	TCCON – TCCON prior	−0.96	2.26

AMTD
5, 4495–4534, 2012

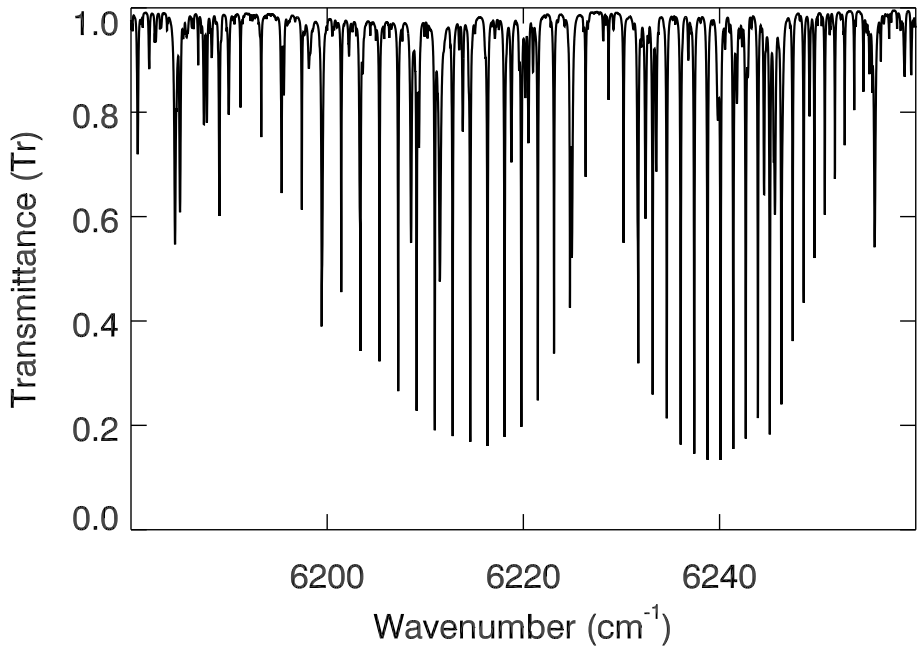

Fig. 1. CO_2 band at 1.6 µm observed on 17 June 2008 by TCCON at Park Falls (Wisconsin) with solar zenith angle of 22.5°.

AMTD
5, 4495–4534, 2012

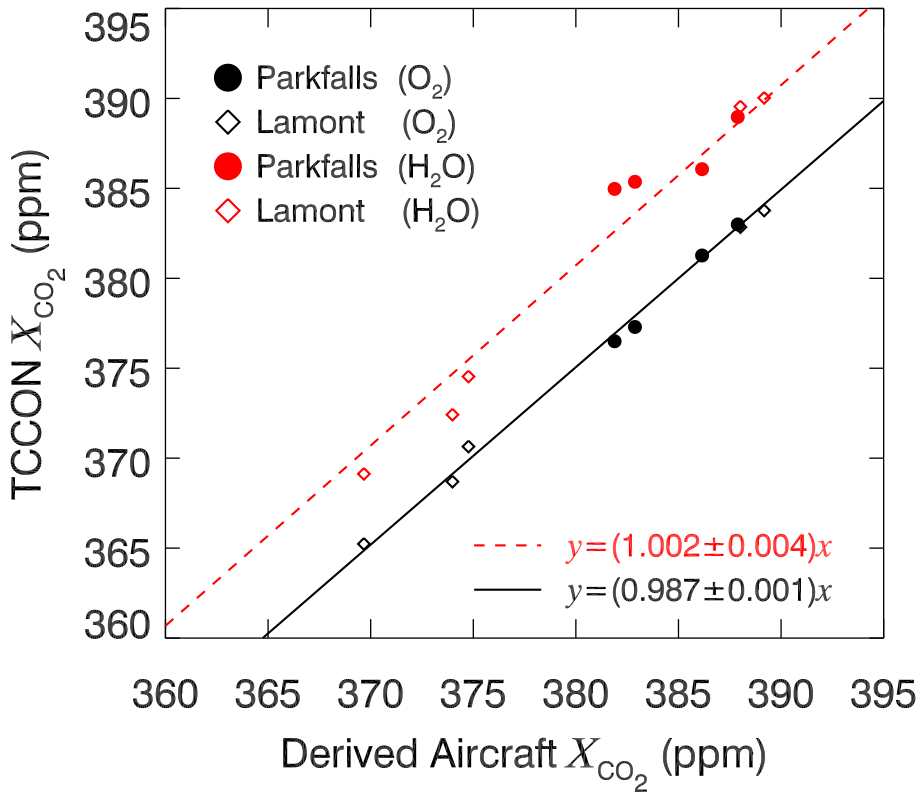

Fig. 2. Comparison of column-averaged CO_2 estimates to derived aircraft column averages. Red points indicate that H_2O is used as dry air standard. Black points indicate that O_2 is used as dry air standard. Dots for Parkfalls site and diamonds for Lamont site. Error bars are not shown in this figure.

AMTD
5, 4495–4534, 2012

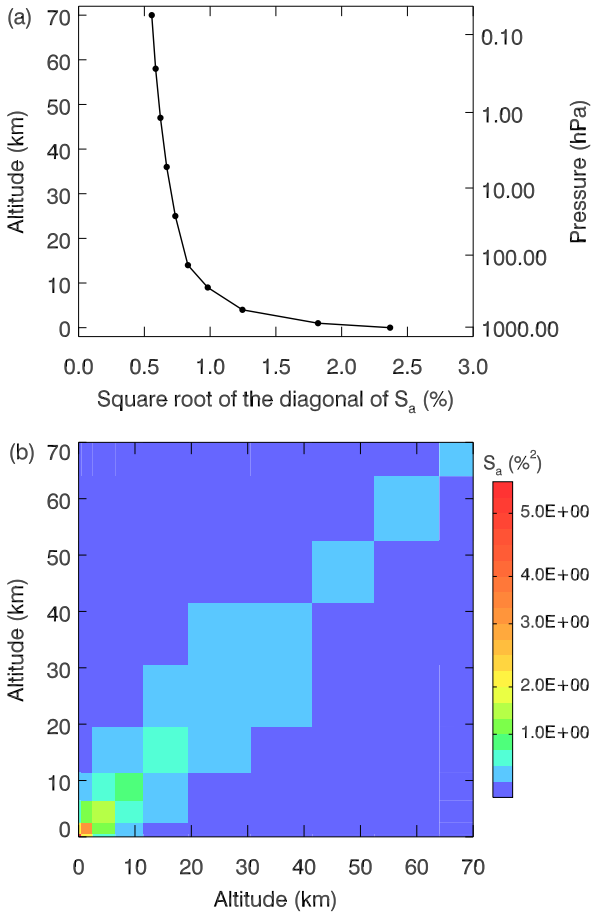

Fig. 3. (a) The square root of the diagonal in CO_2 covariance matrix. **(b)** The 2-D plot of the CO_2 covariance matrix.

AMTD
5, 4495–4534, 2012

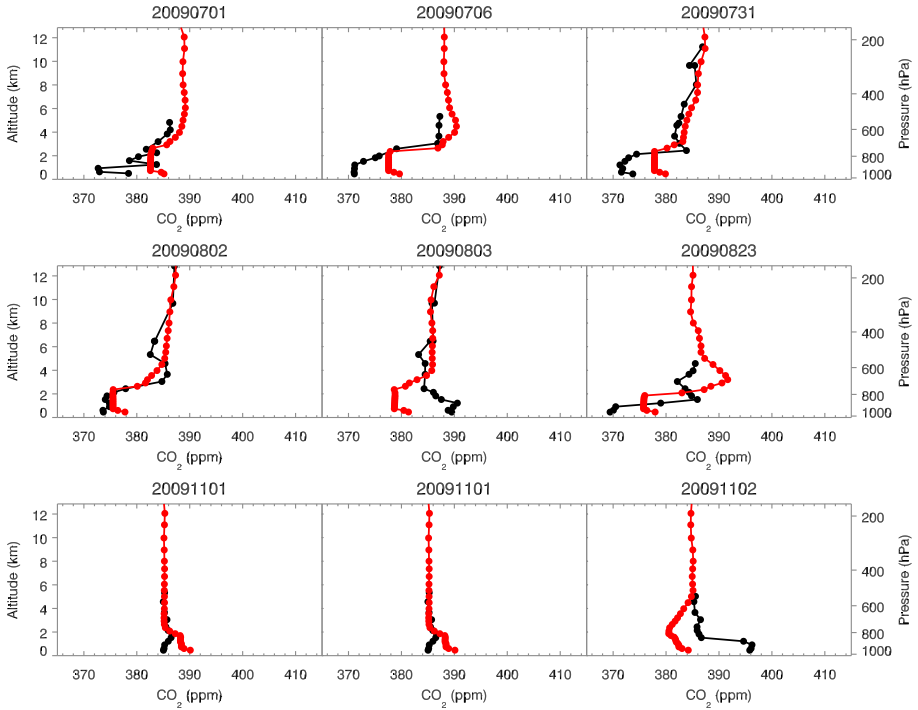

Fig. 4. Samples of CO_2 profiles measured by aircraft (black) and TES Geos-Chem assimilation (red) at SGP.

AMTD
5, 4495–4534, 2012

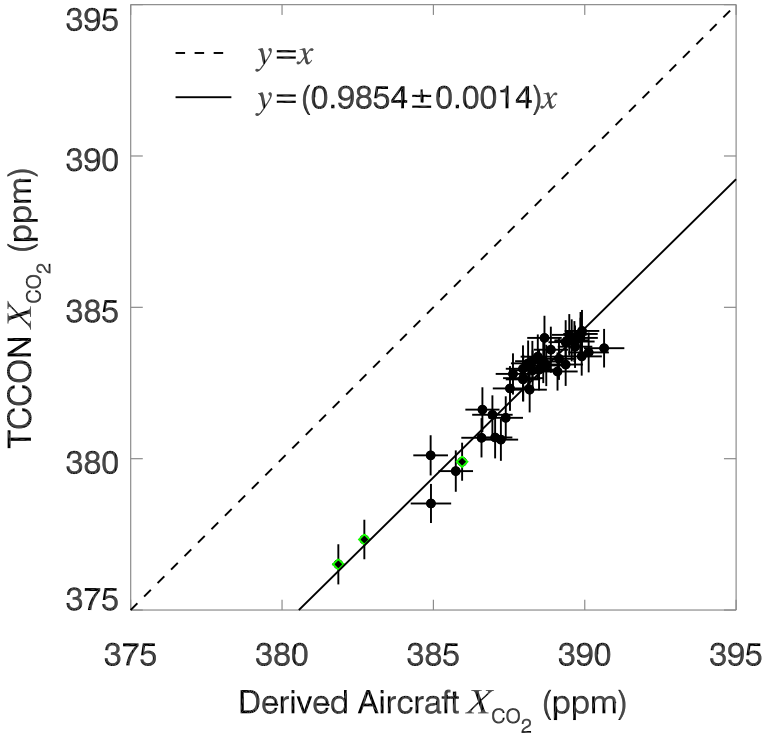

Fig. 5. Comparison of total column-averaged CO_2 from TCCON profile retrievals to that derived from aircraft. Black dots indicate comparison of TCCON estimates to aircraft that measure up to 6 km. Green dots are comparison of TCCON estimates to the three aircraft profiles that measure up to 12 km.

AMTD
5, 4495–4534, 2012

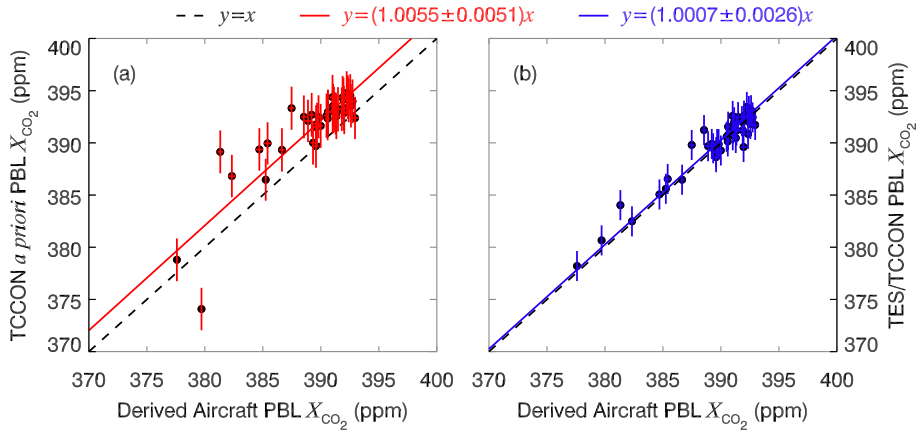

Fig. 6. (a) Comparison of PBL CO_2 estimates derived from integrating from surface to 600 hPa by TCCON a priori and aircraft. **(b)** Comparison of PBL CO_2 estimates derived from TCCON and TES with aircraft.

AMTD
5, 4495–4534, 2012

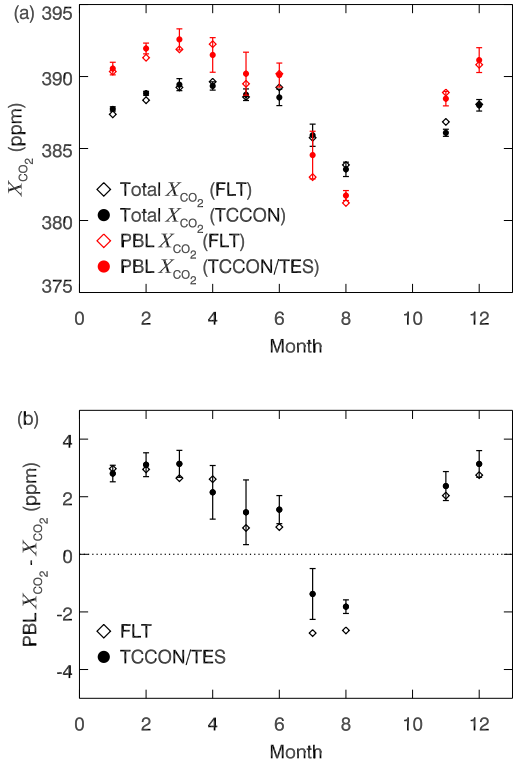

Fig. 7. (a) Monthly mean XCO2 for total column and PBL CO_2 in 2009 at Lamont. Aircraft data (FLT) are indicated by diamonds (black for total XCO2; red for PBL XCO2) and TCCON or TCCON/TES estimates are indicated by black or red dots + error bars. **(b)** The difference of PBL CO_2 and total column-averaged CO_2 by flight (diamonds) and by TCCON/TES (dots). Error bars are the standard deviation of the monthly estimates.

AMTD
5, 4495–4534, 2012